Supporting Information

Alfaro *et al.* 10.1073/pnas.0803437105

SI Materials and Methods

Materials

Antibodies. Ly-6A/E/ScaI (clone E13–161.7; BD Pharmigen, 553336), CD11b (clone M1/70; BioLegend 101215) or (cloneM1/70; R&D Systems, MAB1124), CD14 (clone biG 53; Alexis ALX-804–499-C100) or (clone TuK4; Caltag Laboratories), CD16/32 (clone 93; eBioscience, 14–0161), CD44 (clone KM81; Cedarlane, CL8944F), CD144 (clone 11D4.1; Fitzgerald, RDI-MCD 144–11D4), CD146 (clone P1H12; Chemicon International, MAB16985), Dkk1(lot GLB01; R&D Systems, AF1096), Sfrp2 (clone 331022; R&D Systems, MAB1169), Wnt3a (clone 217804; R&D Systems, MAB1324), CD31/platelet endothelial cell adhesion molecule-1 (PECAM-1; clone 557355, PharMingen)

Recombinant Proteins. Dkk1 (lot MCB056011; R&D Systems; catalog no. 1765-DK), PDGF-BB (lot BW17; R&D Systems; catalog no. 220-BB), Sfrp2 (R&D Systems; catalog no. 1169-FR), Sfrp3 (R&D Systems; catalog no. 592-FR), Sfrp4 (R&D Systems; catalog no. 1827-SF), Wnt3a (R&D Systems; catalog no. 1324-WN).

cDNA. Sfrp2 (GenBank accession no. BC014722; ATCC; catalog no. 6465272), Wnt3a (GenBank accession no. X56842; ATCC; catalog no. MBA-176), Dkk1 (GenBank accession no. NM012242; E. Lee, Vanderbilt University)

Animals/Surgical Interventions

Repair/Granulation Tissue Stimulation. To compare MSCs from disparate strains without inciting immune mediated rejection, we used the immunodeficient NOD/SCID strain. Some of the NOD/SCID mice also contained an inactivating mutation in the β-gluc gene to enable precise tracking and quantification of exogenous MSCs (1). β-gluc is a lysosomal enzyme that is expressed in all cell types, including human and mouse BM-derived cells. Upon transplantation into a β-gluc-negative host, cells from normal human and/or murine donors (e.g., exogenously added MSCs) can be identified by virtue of their β-gluc expression at a level of single cell sensitivity by quantitative biochemical or histochemical techniques (1–4). Biochemical measure of β-gluc activity correlated with MSC numbers in sponges in a linear manner (data not shown). Each mouse was implanted with multiple sponges (PBS, WT, MRL or various WT-MSC transducts, sFRP2, GFP, or Dkk1-MSCs) to enable evaluation of sponge repair tissues mediated by MSCs/PBS within the same animal and between experimental mice Animals were taken down between 14 and 21 days after sponge implantation. *Myocardial Infarction:* Since functional outcome or infarct size was not significantly different between WT-MSCs and GFP-MSCs, the data were combined for subsequent comparisons. Postsurgical echocardiograms were obtained on unsedated mice from 2-D guided M-mode images (100 frames/sec) with 3 consecutive cardiac cycles measured to obtain the mean cardiac dimensions. Echocardiograms were read blinded using short axis and a parasternal long-axis views with the leading edge method. To measure infarct size, excised hearts were immersion-fixed in 10% buffered formalin for 24 h and transferred to 70% ethanol after which serial sections through the ventricles were made parallel to the atrioventricular groove. The samples were then processed for light microscopy. Paraffin sections cut at 6 μm were stained with H & E and Masson trichrome. Infarcted areas on trichrome-stained slides were quantified in all sections as the percentage of left ventricle that exhibits myocyte replacement by scar using Image Pro software (Media Cybernetics) (5).

Cells. Primary MSC cells were generated from pooled BM from $n = 3$ mice. Two independently isolated primary MSCs were used for both WT and MRL experiments and representative data presented. The immunophenotype of MSCs was assessed for the presence of CD44 and LY6A/E/ScaI by FACS analysis on a LSMII flow cytometer and subsequently analyzed using FACS-Diva v5.02 software (Becton Dickinson). Isotype control antibodies were used to establish quadrants. Nonviable cells, identified by 7-aminoactinomycin D (7-AAD) (Molecular Probes) staining, were excluded. Absence of CD45, CD14, CD11b, CD16/32, CD144, and CD146 expression was confirmed by immunofluorescence microscopy of acetone-fixed coverslips (data not shown) using a Zeiss Axioplan microscope as previously reported (4). MSCs were maintained in DMEM-LG (Biowhittaker), 10% defined FBS (HyClone, Mediatech; Cellgro), antibiotics, fungizone and 20 μg/ml PDGF. BrdU Cell Proliferation Assay (Calbiochem) was used to quantify the proliferation of the MSCs. Briefly, 0.5×10^3 cells were seeded on 96 well plates and serum starved for 6 h. The cells were grown in full media for the next 12 h before the addition of BrdU for 16 h before analysis. β-gluc enzyme specific activity of sponge homogenates was measured as described in ref. 1 and was normalized to DNA content using the FluoReporter Blue Fluorometric dsDNA Quantitation Kit (Molecular Probes) according to manufacturer's instructions.

RNA Isolation/Microarray. RNA was isolated using TRIZOL reagent (Invitrogen) and purified according to manufacturer's instructions using RNeasy Mini Kit (Qiagen). The Affymetrix One Cycle reaction was initiated using a sample mix of high-quality total RNA, polyA spike in controls (included in kit), 50 μM T7 dT oligo, and H_2O. First strand synthesis mix (5X first strand buffer, 0.1 M DTT, 10 mM dNTP, SuperScript II) is added to the sample mix and incubated at 42°C for 1 h, with cooling to 4°C for 5 min. Subsequently, second strand synthesis mix (second strand buffer mix, 10 mM dNTP mix, E. Coli DNA ligase, E. Coli DNA polymerase I, E. Coli Rnase H) is added to the sample mix, and incubated at 16°C for 2 h. At this point, T4 DNA polymerase is introduced, and incubated at 16°C for 5 min, followed by the addition of 0.5M EDTA to stop the reaction. The samples are then purified by binding to and elution from a Qiagen column. The resulting cDNA is labeled and amplified in an IVT reaction using biotinylated nucleotides. The reaction is done by adding the purified cDNA to labeling mix (10X IVT labeling buffer, IVT labeling NTP mix, IVT labeling enzyme mix, H_2O) and incubating 16 h at 37°C. The biotinylated cRNA molecules are purified by binding and eluting from a Qiagen column. After quantification, 20 μg of the reaction products are fragmented using fragmentation buffer and H_2O, and incubated at 94°C for 35 min. Fragmentation reaction products and non-fragmented cRNA samples are compared with bioanalysis to ensure that fragmentation is complete. Fragmented samples were then hybridized to the chip Mouse 430 2.0 array, stained and scanned (Affymetrix GeneChip Scanner 3000 7G with AutoLoader). Analysis of the probe levels was performed using robust multi array average (RMA) normalization. GeneSpring 7.3 (Agilent Technologies) was used for the analysis and visualization of the RMA-transformed data. t test with confidence level of $P < 0.05$ was used. Duplicates of each sample were run.

Real-Time RT-PCR. First-strand cDNA was synthesized with reverse transcriptase and oligo(dT) priming (iScript, BioRad) from total RNA. Real-time RT-PCR was performed in triplicate for each sample with a commercial system (iCycler; BioRad) and fluorescence detection (FastStart SYBR Green; Roche). Each reaction was normalized against 18S. Primer sequences can be found in Table S2.

Transduction. cDNAs of interest were subcloned into LZRS-MS-IRES-GFP retroviral expression vector (Alyssa Weaver, Vanderbilt). Phoenix 293 packaging cells (Alyssa Weaver, Vanderbilt) were maintained in DMEM with 10% FCS. Phoenix 293 cell transfection, viral harvest, and target cell transduction were as described in ref. 6. Viral supernatant was collected and passed through a 0.2 μm filter. MSCs were infected with LZRS-cDNA-GFP or LZRS-GFP as control. Due to varied transduction efficiencies (see Table S3) GFP-positive cells were sorted using BDFACS Aria at least 2 days after transduction. This process was repeated throughout the course of the experiments.

Histochemistry and Morphometry. PVA Sponges were cut in half and embedded with cut surface down for histology. The other half was frozen for quantitative biochemical analysis. Immunohistochemistry for CD31 was performed as described in ref. 1. Images were photographed with a CoolSNAP Hq CCD camera (Photometrics). Microvascular density was performed by obtaining 10 digital images at defined magnification taken at random from each section. Immunostained sections were imaged with a digital camera (Pixera, Los Gatos, CA) and the images processed using Scion Image software to automatically measure total immunopositive areas. The area of tissue for each field was quantified using MetaMorph (Molecular Devices) by outlining tissue and calculating total area per field. For confocal analysis, LSM510 (Zeiss) microscope was used to capture 0.8-μm optical slices (z-stack); the images were analyzed with Metamorph v5.0 (Universal Imaging).

Differentiation. MSCs plated at minimal cell density (3–5%) on coverslips were grown in differentiating media for 2 weeks with fresh media added every 4 days (7). Cells directed toward an adipogenic lineage (10 μM dexamethasone (dex), 10 μg/ml insulin, 100 μg/ml IBMX) were fixed for 30 min with 10% buffered formalin and stained with 0.21% Oil Red O (Sigma-Aldrich). Cells undergoing chondrogenic (100 μM dex, 0.01 μg/ml TGF-β1) and osteogenic (100 μM dex, 0.1 mM ascorbic acid, 10 nM β-glycerophosphate) differentiation were fixed for 15 min with 100% ethanol and stained with Alcian Blue pH 1.0 and 0.2% Alizarin Red (Sigma-Aldrich), respectively. To confirm chondrogenic commitment, dimethyl methylene blue (dMMB, Sigma) was used as a metachromatic dye that allows histochemical detection and quantification of sulfated proteoglycans within the cell lysates as described in ref. 8. Briefly, cells were washed with 1X PBS and scraped after adding lysis buffer. The dMMB solution (16 mg of dMMB in 1 L of H_20 containing 3.04 g of glycine, 2.37 g of NaCl and 95 mL of 0.1 M HCl, pH 3.0) was mixed with 5 μL of cell lysate and absorbance was read at 525 nm. The calculated proteoglycan content was normalized to DNA content.

Canonical Wnt Signaling. To assess intrinsic Wnt signaling, MSCs were transiently transfected using Lipofectamine 2000 (Invitrogen) with the luciferase reporter construct containing 8 copies of optimal (SuperTOPFlash) or mutant (control, superFOPFlash) TCF/LEF transcription factor binding sites upstream of luciferase, plus a CMV-driven β-galactosidase (β-gal) reporter to control for transfection efficiency. Twenty-four hours after transfection, cells were collected and luciferase activity was measured with the Dual Luciferase Assay (Promega) and reporter expression was normalized to cotransfected β-gal activity (Pierce). Wnt signaling in conditioned media was assessed using HEK 293 cells that were stably transfected with SuperTOPFlash reporter. Specified numbers of HEK cells were seeded onto 48-well plates. After 24 h, conditioned media or recombinant proteins were added and luciferase activity measured after 8 h.

Dkk1 ELISA. A 96-well enzyme immunoassay kit for human Dkk1 detection was purchased from Assay Designs (catalog no. 900–151). The assay was performed according to manufacturer's instructions. Briefly, conditioned media from the transduced cells was diluted 1:2,500 and 1:5,000 in the assay buffer containing protease inhibitors; 100 μL of each sample was added to the precoated wells in the kit, in triplicate. Serial dilutions of the provided lyophilized Dkk1 standard were performed and 100 μL of each dilution was added to the wells, in duplicate. The samples were incubated for 1 h at room temperature on a plate shaker. After washing, 100 μL of primary antibody was added and another 1 h long incubation elapsed. Secondary antibody was added after a washing step. After washing, 100 μL of substrate solution was added to the wells and incubated for 30 min at which point 100 μL of a stop solution was added to each well. The optical density was ready at 450 nm. The concentration of each sample was determined by the use of equation of the best fit line from the standard samples.

sFRP2 Knockdown by Lentiviral Transduction of shRNA. sFRP2 was knocked down of MRL-MSCs by transduction with a lentivirus containing short hairpin RNA (shRNA) construct targeting sFRP2 coding sequence. Three different target constructs were tested. Mission Lentiviral Transduction Particles were purchased from Sigma (SHVRS) along with the control transduction particles (SHC002V). Transduction and selection of clones was done following manufacturer's instructions. Briefly, 1.6×10^4 cells per well were seeded in a 96-well plate and incubated 20 h. Fresh media with 8 μg/ml hexadimethrine bromide was added before the addition of the lentiviral particles at a multiplicity of infection of 5. The cells were incubated with the lentivirus overnight and fresh media was added the following day. After 24 h, media containing 7.5 μg/ml puromycin was added and replaced every 3–4 days. MRL-MSCs transduced with lentiviral control construct (control shRNA) and MRL-MSCs with shRNA knockdown of sFRP2 (MRL-kd-sFRP2) were selected by puromycin resistance and analyzed by immunoblot for specific protein expression.

Immunoblot. Cellular proteins were extracted with RIPA buffer. After BCA Protein Assay (Pierce) proteins were resolved by SDS/PAGE and transferred to nitrocellulose. Membranes were incubated with primary antibody diluted in 5% milk-TBST at 4°C overnight. Species-specific secondary antibodies conjugated to HRP were used and chemiluminescence (PerkinElmer, NEL104) was detected by film. ImageJ version 1.38x (National Institutes of Health) software was used for densitometry analysis of the appropriate lanes; values are normalized to β-actin loading control.

Statistical Analysis. The statistical significance between experimental groups and control was determined by paired or unpaired Student's t test or ANOVA followed by Bonferroni post test or Newman-Keuls multiple comparison test as designated using GraphPad Prism. $P \leq 0.05$ was considered statistically significant and marked in figures.

1. Young PP, Hofling AA, Sands MS (2002) VEGF increases engraftment of bone marrow-derived endothelial progenitor cells (EPCs) into vasculature of newborn murine recipients. *Proc Natl Acad Sci, USA* 99:11951–11956.
2. Soper BW, Duffy TM, Vogler C, Barker JE (1999) A genetically myeloablated MPS VII model detects the expansion and curative properties of as few as 100 enriched murine stem cells. *Exp Hematol* 27:1691–1704.
3. Young PP, Vogler C, Hofling AA, Sands MS (2003) Biodistribution and efficacy of donor lymphocytes in a murine model of lysosomal storage disease. *Mol Ther* 7:52–61.
4. Teleron AA, Carlson B, Young PP (2004) Blood donor white blood cell reduction filters as a source of human peripheral blood-derived endothelial progenitor cells. *Transfusion* 45:21–25.
5. Pfeffer MA, *et al.* (1979) Myocardial infarct size and ventricular function in rats. *Circ Res* 44:503–512.
6. Ireton RC, *et al.* (2002) A novel role for p120 catenin in E-cadherin function. *J Cell Biol* 159:465–476.
7. Tropel P, *et al.* (2004) Isolation and characterisation of mesenchymal stem cells from adult mouse bone marrow. *Exp cell Res* 295:395–406.
8. Farndale RW, Buttle DJ, Barrett AJ (1986) Improved quantitation and discrimination of sulphaged glycosaminoglycans by use of dimethylmethylene blue. *Biochimica et Biophysica Acta* 883:173–177.

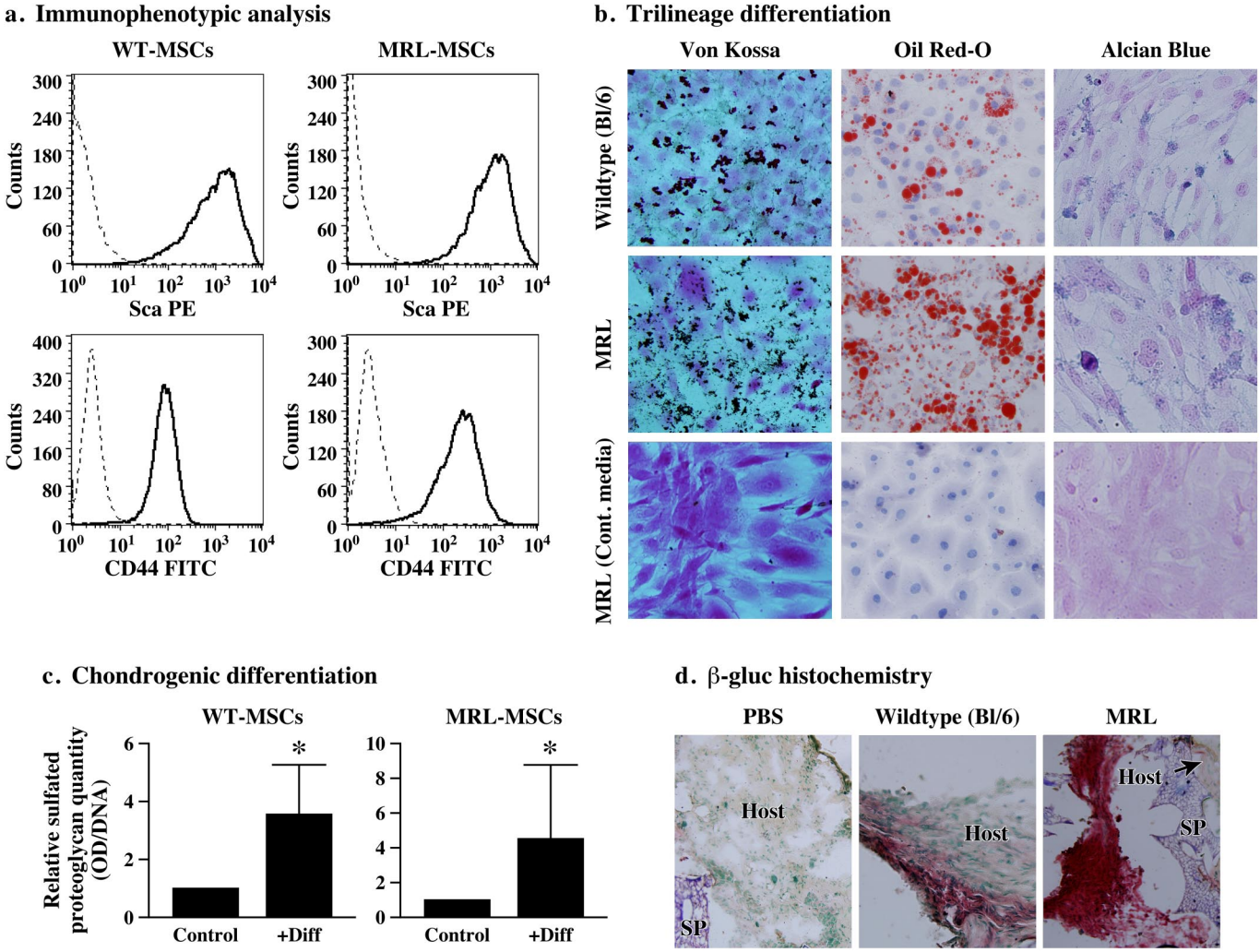

Fig. S1. Characterization of WT (Bl/6) and MRL (MRL/MpJ) MSCs. (*a*) Isolated MSCs were shown to express MSC markers, including CD44 and Sca1 (dark line), by FACS. Cells stained with isotype antibodies are shown in dotted gray line. (*b*) MSC multipotency was confirmed by positive differentiation into adipocytes, osteocytes and chondrocytes. MSCs maintained in control media where differentiation was not induced also are shown. (*c*) Graphical representation of quantified sulfated proteoglycans in differentiated cells. Fold change over non-differentiated MSCs, normalized to DNA content. (*d*) Photomicrograph of β-gluc histochemical analysis of PBS, WT- and MRL-MSC-loaded sponge cryosection showing abundant engraftment of MSCs within granulation tissue (β-gluc+, red) and adjacent β-gluc negative host tissue. SP, sponge matrix.

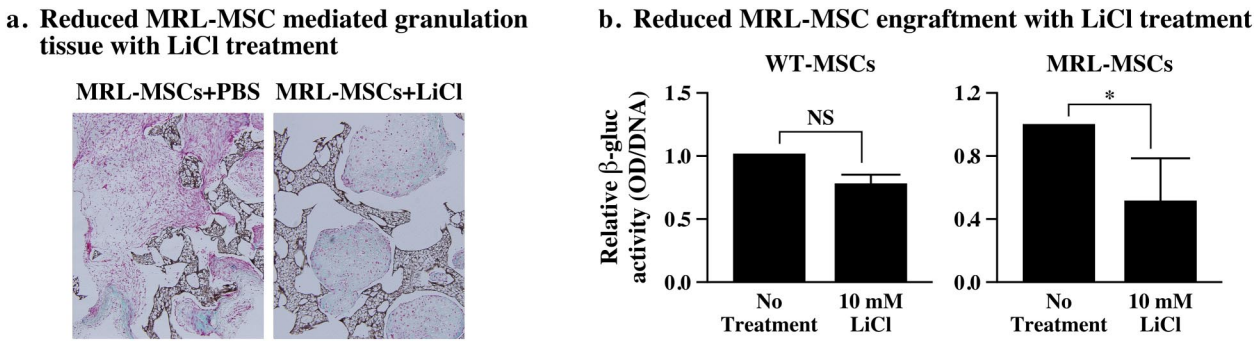

Fig. S2. Effects of Wnt signaling on MSCs. (*a*) Representative low power Trichrome images show decreased granulation tissue in MRL-MSC-loaded sponges treated with Lithium Chloride (LiCl) vs. PBS control. Note that LiCl (Wnt activation) promoted in vivo differentiation of MSCs into cartilage. (*b*) Graphical representation of β-glucuronidase activity as a marker of MSC engraftment in the presence or absence of LiCl treatment. Two-tailed, unpaired student's *t* test was performed to compare the effects of LiCl on the levels of engraftment. Asterisk designates statistical significance of $P \leq 0.05$. NS, no statistical difference.

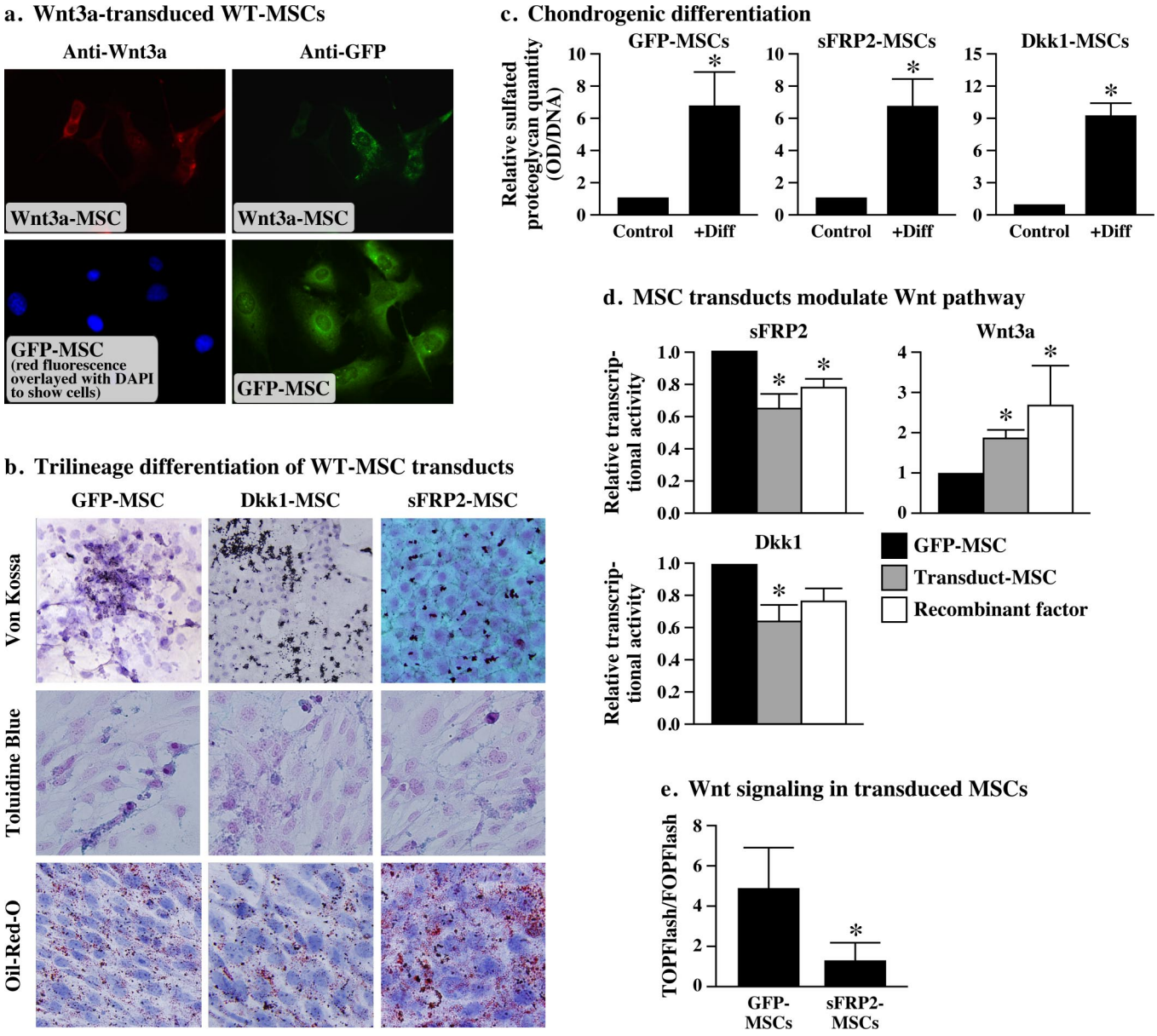

Fig. S3. Characterization of MSCs transduced with Wnt pathway constituents. (*a*) GFP-sorted WT (Bl/6)-derived MSCs transduced with Wnt3a IRES GFP (Wnt3a-MSCs) and vector control (GFP-MSCs), were assessed by immunofluorescence to confirm GFP/Wnt3a coexpression. (*b*) Multipotency of MSC transducts was confirmed by positive differentiation into adipocytes, osteocytes and chondrocytes. (*c*) Graphical representation of sulfated glycosaminoglycans as measurement of chondrogenic differentiation. Fold change over non-differentiated transduced MSCs, normalized to DNA content. (*d*) Luciferase activity in HEK cells stably transfected with TOPFlash reporter after treatment with conditioned media from designated MSC transducts or GFP-MSC, as baseline. 50 ng/ml Wnt3a, 100 ng/ml Dkk1, or sFRP2 recombinant proteins were used as positive controls. The results were the average of the fold change from 3 independent experiments performed in duplicate. (*e*) Basal normalized luciferase activity as a measurement of canonical Wnt signaling in transduced MSCs. The effect of sFRP2 was assessed by transfecting sFRP2-MSCs and GFP-MSCs with TOP/FOPFlash reporter constructs.

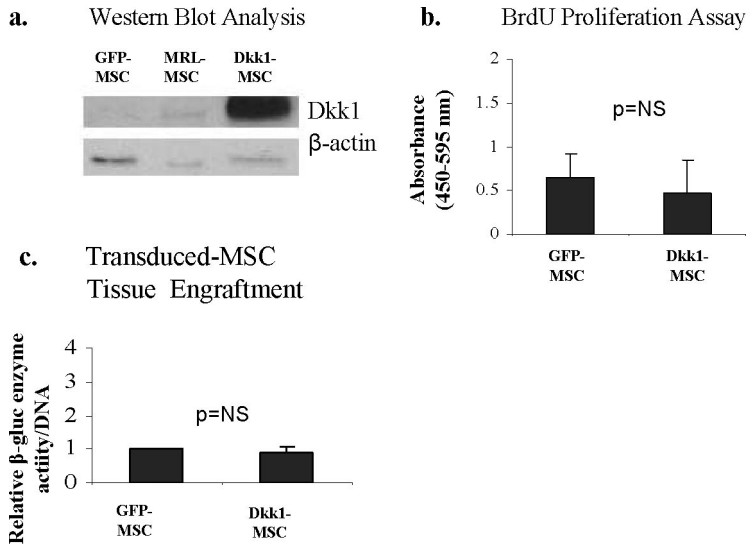

Fig. S4. Wnt inhibition of murine MSCs through Dkk1 does not promote MSC proliferation and engraftment. (*a*) WT-MSCs were retrovirally transduced to express Dkk1 linked to an IRES GFP (Dkk1-MSCs). Transduced cells were sorted for GFP expression and analyzed by immunoblot for specific protein expression. Dkk-1 levels in conditioned media from transduced cells were 1.29 $\pm$ 0.11 μg/ml and undetectable in GFP-MSCs. WT-MSCs transduced with vector containing GFP alone (GFP-MSC) were also sorted in parallel. (*b*) Cell proliferation assay. (*c*) β-gluc specific activity normalized to total cellular DNA content of paired GFP-MSC- or Dkk1-MSC-loaded granulation tissue. One way Anova with Bonferrroni correction was used to compare data between GFP-MSC and Dkk1-MSC.

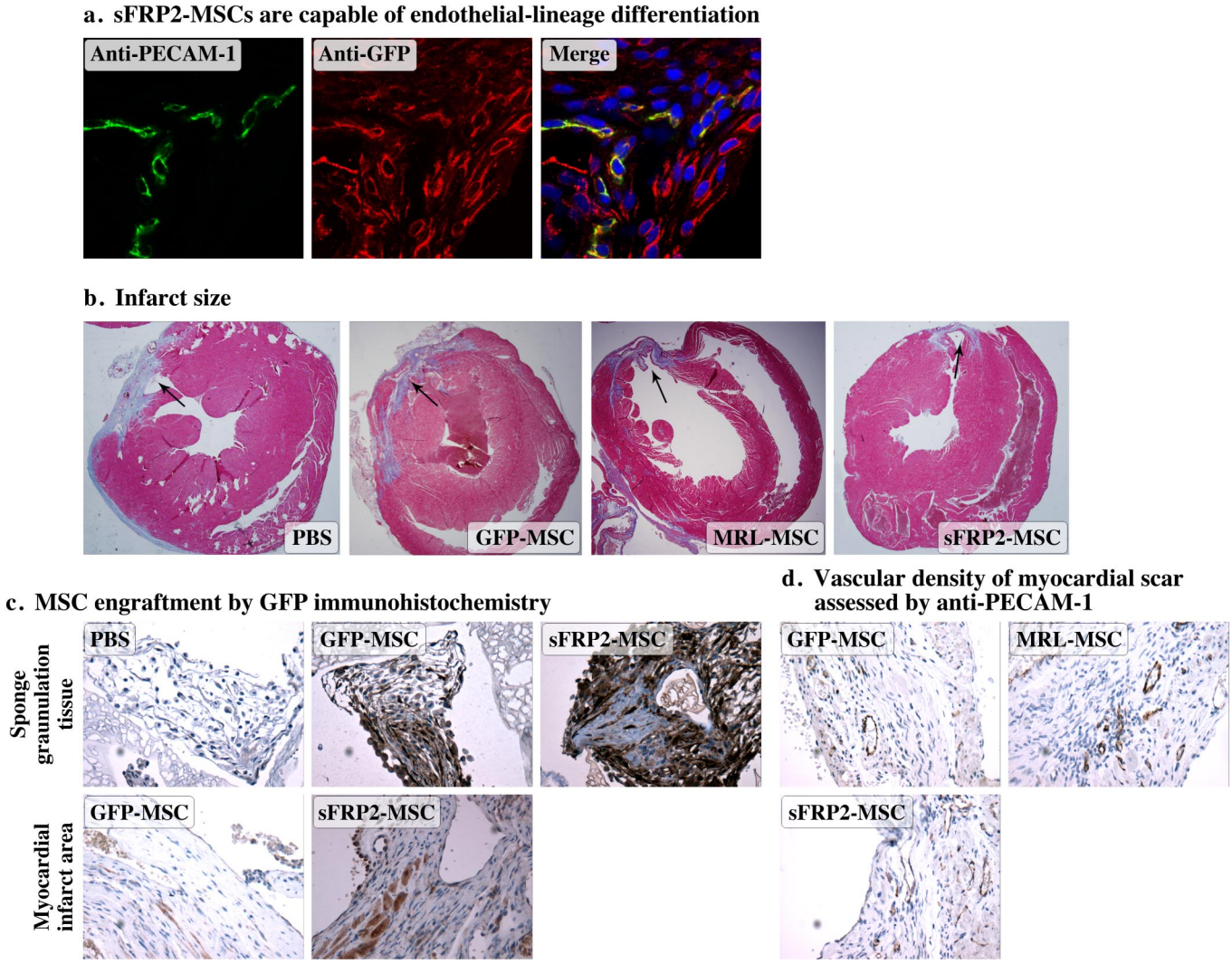

Fig. S5. MSC-mediated cardiac therapy. (*a*) Representative Z plane shows high degree of colocalization of microvascular endothelial cells (anti-PECAM, green) and the sFRP2-MSC marker, GFP (red). Fluorescent images were acquired by confocal fluorescent microscopy with 60x lens. DAPI staining of the same slide shows the location of the nuclei. (*b*) Representative Masson trichrome-stained sections of hearts from mice 30 days after receiving PBS, GFP-MSC, MRL-MSC or sFRP2-MSC after coronary vessel ligation. MRL and sFRP2-MSC treated hearts had smaller infarcts with less collagen deposition (blue staining in trichrome) and more muscle (increased red staining). (*c*) Engraftment of sFRP2- and GFP-MSCs was assessed by immunostaining with anti-GFP (brown). sFRP2-MSC showed increased engraftment in both models, however, there was significantly higher engraftment within sponge granulation tissues than in healed myocardial scar. (*d*) Representative immunostained sections of myocardial scar using anti-PECAM-1 to designate vascular density among experimental cohorts.

Table S1. Wnt pathway inhibitors are up-regulated and Wnt downstream targets are down-regulated in MRL-MSCs

Gene name	Fold Change	*P*	*n*
Wnt pathway inhibitors			
Secreted frizzled-related sequence protein 2 (Sfrp2)	251.8 ± 346	$P \leq 0.05$	$n = 9$
Secreted frizzled-related sequence protein 4 (Sfrp4)	31.61 ± 34.97	$P \leq 0.05$	$n = 6$
Dickkopf homolog 1 (Dkk1)	ND	NA	NA
Wnt Downstream Targets			
Axin2	0.1998 ± 0.1364	$P < 0.01$	$n = 7$
High mobility group box protein (Sox2)	0.0785 ± 0.0410	$P < 0.01$	$n = 6$
Cyclin D1	0.2119 ± 0.1316	$P < 0.01$	$n = 8$

Gene expression was analyzed through quantitative real time RT-PCR. Fold changes, *P* values, and number of runs are specified for each gene. ND, not detected; NA, not applicable.

Table S2. Quantitative real time RT-PCR primers

Gene	Forward primer	Reverse primer
18S	CGCCGCTAGAGGTGAAATTCT	GAACCTCCGACTTTCGTTCCT
Axin2	GGACAGTAGCGTAGATGGAG	CGGAAAATGAGGTAGAGACA
Cyclin D1	CTGGTGTTTGGAAGTAGGAA	GTTTAAAAGCCTCCTGTGTG
Sfrp2	ATGGAAACCCTTTGTAAAAATGACT	TCTTGCTCTTTGTCTCCAGGATGAT
Sfrp4	TTGATGCTGACTGTAAACGTCTGAG	CCTCTGGACGGCTTTTATTTTGGCA
Sox2	GGAGAGTAGGAAAAATCTGATAATG	ATCTCTCATAAAAGTTTTCTAGTCG
Wnt3a	CCTCGGAGATGGTGGTAGA	GTTAGGTTCGCAGAAGTTGG

18S was used as an internal control. PCR products range in size between 75 and 200 bp.

Table S3. Transduction characterizations

Transduct	No. of transductions	Average transduction efficiency, %	Standard deviation, %
GFP	4	50.64	± 24.03
Dkk1	2	85.5	± 14.14
Sfrp2	4	48.12	± 9.61
Wnt3a	6	26.15	± 8.95

Data shows that our experiments were generated from multiple transductions with varying levels of efficiency. The transduction efficiency for sFRP2-MSCs and GFP-MSCs was ≈50%.

Table S4. Transduction characterizations

Clone	Fold change	*P*
Control A	1	NA
Control B	1	NA
75B	0.08 ± 0.03	$P = 0.048$
76B	0.57 ± 0.20	$P = 0.117$
77C	0.035 ± 0.02	$P = 0.059$

Real-time RT-PCR analysis of different constructs and control MRL-MSCs. All reactions were carried out in triplicate and the results represent the average ± SD of three independent experiments. Two-tailed paired Student's *t* test was performed.

Table S5. sFRP2-MSCs express several angiogenic factors

Gene ID	Gene Name	Fold Change in sFRP2-MSC
1422516_a_at	Fibp (Fibroblast growth factor intracellular binding protein)	2.2
1433489_s_at	FfgR2 (Fibroblast growth factor receptor 2)	2.1
1419417_at	VegfC (Vascular endothelial growth factor C)	2.3
1418711_at	Pdgfa (Platelet-derived growth factor, alpha)	2.4
1417148_at	Pdgfrb (Platelet derived growth factor receptor, beta polypeptide)	2.6
1421919_a_at	Ccr9 (Chemokine [C-C motif] receptor 9)	11.9
1450652_at	Ctsk (Cathepsin K)	16.7
1450029_s_at	Itga9 (Integrin alpha 9)	2.3
1455158_at	Itga3 (Integrin alpha 3)	2.7
1425039_at	Itgbl1 (Integrin beta-like 1)	5.7
1454966_at	Itga8 (Integrin alpha 8)	4.5
1423268_at	Itga5 (Integrin alpha 5)	3.3
1446180_at	Lamb1–1 (Laminin beta subunit-1)	5.0
1446534_at	Angptl2 (Angiopoietin-like 2)	2.5
1417130_s_at	Angptl4 (Angiopoietin-like 4)	2.2
1419671_a_at	Il17rc (Interleukin 17 receptor C)	2.5
1421670_a_at	Irak4 (Interleukin-1 receptor-associated kinase 4)	2.1
1435040_at	Irak3 (Interleukin-1 receptor-associated kinase 3)	3.6
1448950_at	Il1r1 (Interleukin 1 receptor, type I)	4.4
1443937_at	Il2rb (Interleukin 2 receptor, beta chain)	21.7
1425145_at	Il1rl1(Interleukin 1 receptor-like 1)	3.2
1416295_a_at	Il2rg (Interleukin 2 receptor, gamma chain)	5.2
1425560_a_at	S100a16 (S100 calcium binding protein A16)	2.3
1448367_at	Sdf4 (Stromal derived factor 4)	3.9

Microarray analysis of sFRP2-MSCs revealed up-regulation of several genes associated with angiogenesis in comparison to GFP-MSCs.